Transactions, **SMiRT-26**
Berlin/Potsdam, Germany, July 10-15, 2022
Special Session

2019-11-11 LE TEIL EARTHQUAKE - THE ULTIMATE MISSING PIECE OF EXPERIENCE FEEDBACK RELATED TO A NUCLEAR POWER PLANT BUILT ON SEISMIC BASE ISOLATION: A REAL EARTHQUAKE

Emmanuel Viallet[1], Julien Berger[2], Paola Traversa[3], Elias El Haber[3], Estelle Hervé-Secourgeon[4], Guillaume Hervé-Secourgeon[4,7], Loic Zuchowski[5], Guillaume Dupuy[6]

[1] Seismic Risk Fellow Expert, EDF, DIPNN/DT, Lyon, France
[2] Earthquake Engineering Proficient Engineer, EDF, DIPNN/DT, Lyon, France
[3] Seismologist PhD, EDF, DIPNN/DI, Aix-en-Provence, France
[4] Research Engineer, PhD, EDF, R&D/EDF-Lab, Paris-Saclay, France
[5] Earthquake Engineering Proficient Engineer, EDF, DIPNN/CNEPE, Tour, France
[6] Seismic Risk Engineer, EDF, DPN/UNIE, Paris, France
[7] Associate Professor, Université Paris-Saclay, CentraleSupélec, CNRS, ENS Paris-Saclay, LMPS - Laboratoire de Mécanique Paris-Saclay, Gif-sur-Yvette, France

ABSTRACT

Cruas Nuclear Power Plant is a three-loop 900 MW Pressurized Water Reactor designed and built at the end of the seventies. At the original stage of the design of French PWRs, EDF has decided to design series of plants, in order to get identical Structures, Systems and Components (SSCs) for the whole series under consideration. However, when Cruas site was selected, both soil conditions and seismic hazard were identified as non-standard design conditions. For this reason, EDF decided to build the plant on seismic base isolation, in order to keep the nuclear island identical to the rest of the series. The base isolation technology used is the so-called “laminated steel-neoprene bearing” that was already largely used in conventional buildings and bridges.

The plant has now almost forty years of operation and no issue has been identified in relation with this laminated steel-neoprene bearing seismic base isolation technology. This technology is therefore matured for use in nuclear industry and supported by Standards that address design and construction as well as manufacturing and maintenance. The only missing piece of experience feedback was the impact of the occurrence of a real earthquake on the plant, in order to give the opportunity to confirm that the design process (already supported by multiple analyses and test campaigns) provides adequate design margins, based on a real full-scale event.

Le Teil magnitude 4.9 (Mw) earthquake occurred on November 11, 2019 at approximately 15 km from Cruas NPP and led to a ground motion shaking between 0.02 and 0.05 g on site (Peak Ground Acceleration, free field). Although this ground motion level is not very high compared to the DBE of the Plant (0.3 g), due to operational procedures, the plant was shut down and post-earthquake inspections were performed before restart. In this context, the objective of this paper is first to introduce Le Teil earthquake in terms of seismological characteristics, then to describe what was done by the operator in the hours, days and weeks after the earthquake, and to present what was observed on site, especially the actual seismic records compared to analyses. Finally, the paper will put forward the current and further actions that are under progress and/or may start in a close future, including international benchmarks in order to share experience feedback and lessons learnt with the largest international community.

INTRODUCTION: STANDARD DESIGN PRINCIPLES FOR FRENCH NPP AND FOCUS ON CRUAS PLANT

Standard design principles for French NPPs

French Nuclear Power Plants (NPPs) currently under operation are Pressurized Water Reactors (PWRs) that have been designed since the 70's. At the time of the design of these plants, EDF decided to follow a standard design approach for series of plants in order to duplicate main Structures, Systems and Components (SSCs) and keep them identical from one site to another belonging to the same series. In this purpose, regarding seismic design, standard conditions were defined, mainly based on soil conditions and seismic hazard, in order to envelope most of the expected sites (that were not yet known at the early design stage). This standard design principle, as illustrated in Figure 1, also shows that at this stage some site-specific conditions were also anticipated (such as non-standard soil conditions or non-standard seismic level) and could be addressed through specific features (such as special foundation systems or seismic base isolation).

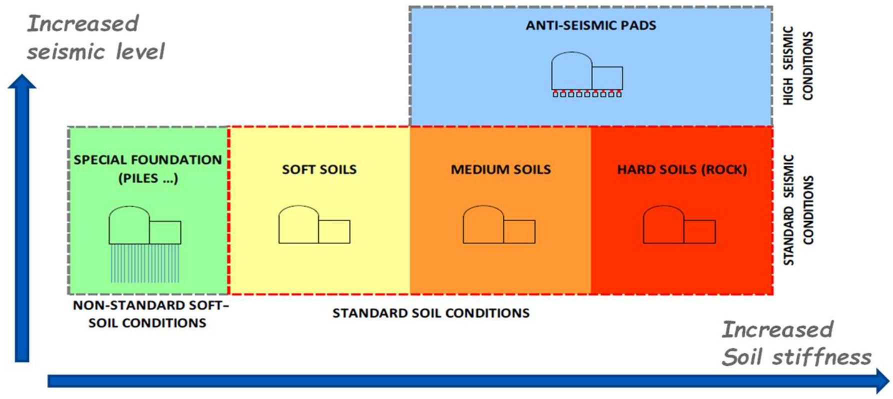

Figure 1. French NPPs standard design principles

Based on these principles, 4 series of plants were designed and built:
- 900 MWe – 3 loop series,
- 1300 MWe – 4 loop series,
- 1450 MWe – 4 loop series,
- EPR 1650 MWe – 4 loop series.

Focus on Cruas NPP

In the case of Cruas NPP, site investigations revealed that the site was mainly composed of limestone with stiff characteristics corresponding to hard rock. In addition, seismic hazard analyses indicated that the site could be subjected to moderate magnitude but near field earthquake with both a higher PGA (0.3g) and a higher frequency content compared with the standard design PGA (0.2g) of the 900 MWe series (see illustration in Figure 4). Then, naturally, EDF decided to build Cruas NPP on seismic base isolation in order to keep the design of all SSCs from the Nuclear Island (NI) identical to the rest of the plants of the series.

In practice, four units are built on Cruas site. A single "upper" basemat supports all NI buildings of a pair of units, as illustrated on Figure 2 (left). This upper basemat is supported by the seismic base isolation system, which is built in a prior phase of the construction, as illustrated in Figure 2 (right).

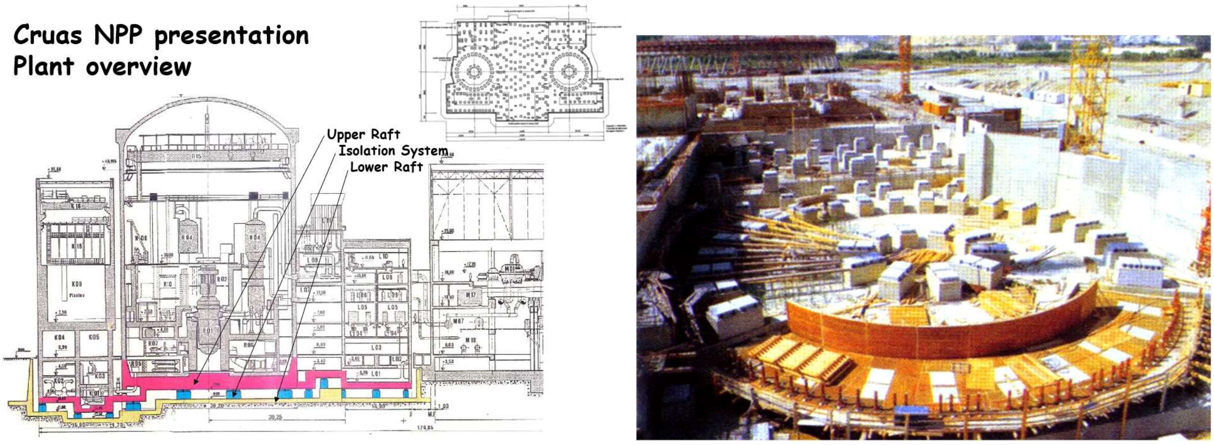

Figure 2. Cruas NPP layout (left) and seismic base isolation system during construction phase (right)

Some more detailed information regarding available seismic base isolation technologies and design approaches for NPPs are provided in an IAEA Tecdoc (IAEA, 2020).

Anti-seismic bearings technology description

The seismic base isolation system which was selected at the time of the design was the so-called laminated steel-neoprene bearing, as described in Figure 3. The main reasons for this choice were i) the well-known technology associated with a large feedback of experience (especially from bridges) and ii) the well-characterized ageing process and kinetic (stiffness of the laminated steel-neoprene bearing increases with time) which allowed to predict long-term evolution since the early design stage.

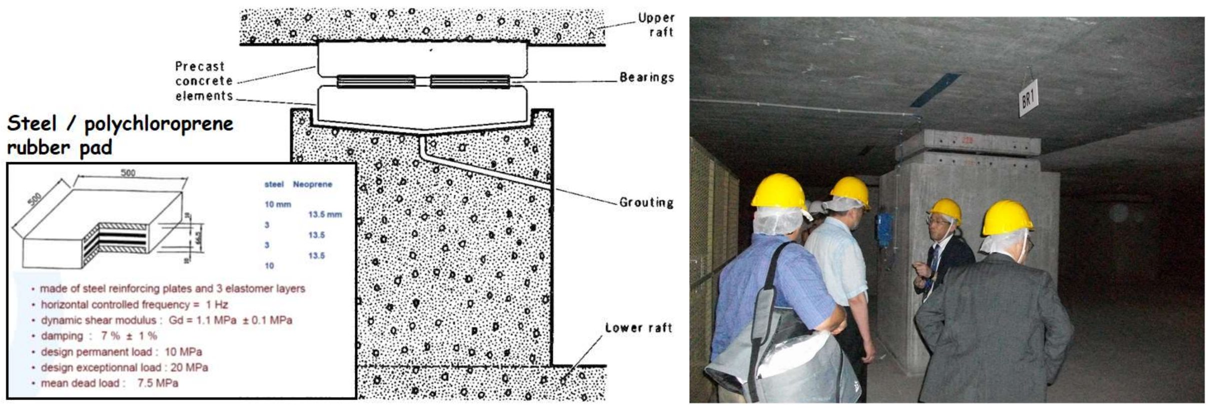

Figure 3. Laminated steel-neoprene bearing description: drawings (left) and actual view (right)

Seismic design principles of Cruas NPP

On the basis of the site conditions and design solutions introduced in the previous sections, the choice was made to design anti-seismic bearings characteristics in order to scale the main horizontal eigenfrequency of the whole isolated system (NI buildings) at 1 Hz for Design Basis Earthquake (DBE) level, including ageing prediction. This target eigenfrequency was selected in order to get a spectral acceleration of the isolated system close to the Peak Ground Acceleration (PGA) of the standard DBE (0.2 g), as illustrated in Figure 4.

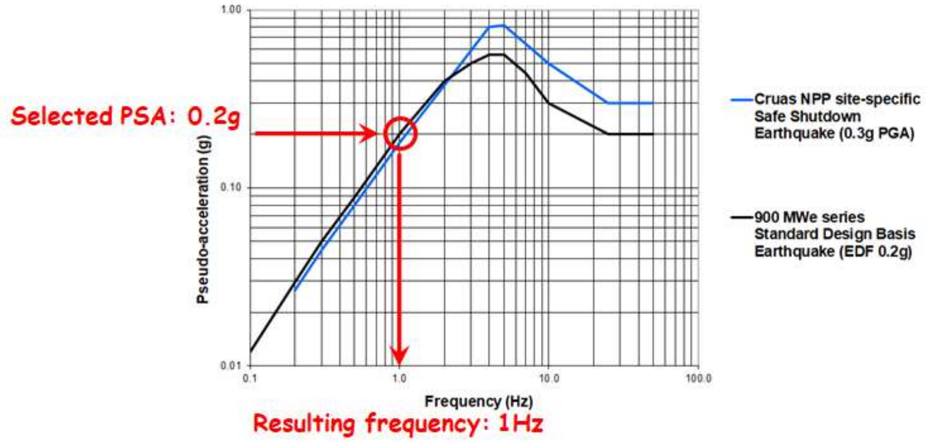

Figure 4. Illustration of Cruas NPP seismic based isolation design principles

2019/11/11 LE TEIL EARTHQUAKE DESCRIPTION

The 2019-11-11 Le Teil earthquake (Mw = 4.9, reverse focal mechanism) occurred in a low to moderate seismicity area within the lower Rhône river valley. In spite of its moderate magnitude, the earthquake caused significant damages to residential buildings in the epicentral area, presumably related to its very shallow focal depth (about 1 to 1.5 km, as described below). The maximum macroseismic intensities reported in the epicentral area are between VII and VIII EMS-98 (Sira et al., 2020).

Satellite radar interferometry images (InSAR) revealed a rupture zone along La Rouvière fault (red line in Figure 5, Ritz et al, 2020).

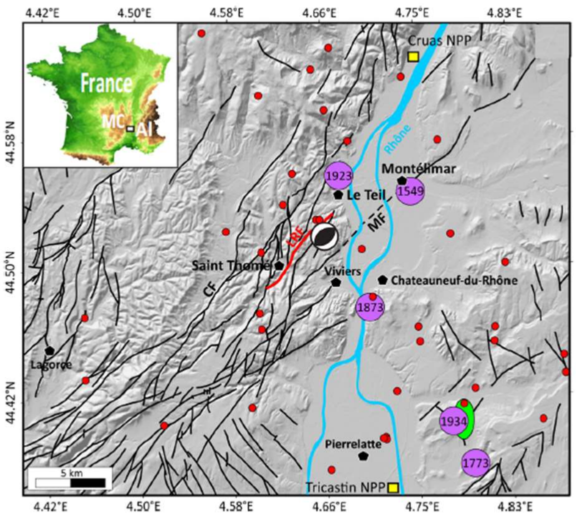

Rupture Parameters	Values
Earthquake magnitude	4.9 (Mw)
Epicenter location	4.6688°, 44.5208°
Hypocenter depth	1 Km
Rupture dimensions	5 x 1.75 Km^2
Strike	50°
Dip	58°
Rake	89°
Stress drop	2 MPa
Rupture velocity (Vr)	1800 m/s
Anelastic attenuation parameters	$Q_0 = 347 \pm 4$
(Q_0 and α)	$\alpha = 0.31 \pm 0.005$
Geometric spreading parameter (β)	1.02 ± 0.02

Figure 5: To the left, Seismotectonic map of the region around the 11 November 2019 Mw 4.9 earthquake. The red and purple circles are instrumental and historical seismicity, respectively; the yellow squares represent the Nuclear Power Plants in the region (Cruas and Tricastin NPP). The black lines are faults from the Aubenas geological map (Elmi et al., 1996) with the La Rouvière Fault (LRF) in red. The shaded DTM is from BD ALTI 25m (IGN); MC and Al in the inset are Massif Central and Alps, respectively. (Figure form Ritz et al., 2020). To the right, the main rupture parameters of the Le Teil earthquake found in the literature and used in the ground motion simulations benchmark (see next sections).

The seismic source of this earthquake was studied in detail (Delouis et al., 2019, Cornou et al., 2021, Ritz et al., 2020, De Novellis et al., 2020, Mordret et al., 2020). The rupture area was very shallow, with a length of ~5km and a width of 1.75 km. The rupture reached the surface, inducing surface deformation, which is unusual for earthquakes of such moderate magnitude. Up to 15 cm of uplift was observed on the SE side of the fault (Delouis et al., 2021). Based on the analysis of the seismological network records, the earthquake hypocenter was located on the NW portion of the La Rouviere fault at a depth in the range of 1−1.5 km (Cornou et al., 2020, Delouis et al., 2021).

The ground motion produced by Le Teil earthquake was widely recorded by the seismic stations of the RESIF consortium national network (RESIF 1995a, 1995b) and by the seismic stations installed at Nuclear Installation sites. Figure 6 shows Peak Ground Accelerations (PGA) recorded by accelerometric and broad-band seismic stations within 500 km as function of distance and Eurocode 8 site classification.

In France, EDF's NPP sites dispose of two different types of seismic instrumentation, with two different goals. On one hand, five sensors constitute the seismic safety monitoring system (EAU), including one free field sensor and four sensors installed within the main structures of the plant (see next section for more details). On the other hand, the RAN seismological network includes at least one accelerometer and one broad-band sensors installed at free-field condition at all NPP. The aim of this latter network is to provide continuous recordings that can be used in seismological analyses and seismic hazard studies.

Cruas NPP is located at 15 km distance from Le Teil epicenter. The RAN broad-band sensor saturated during the shaking, while the accelerometer provides the closest high-quality record of the Le Teil earthquake ground motion.

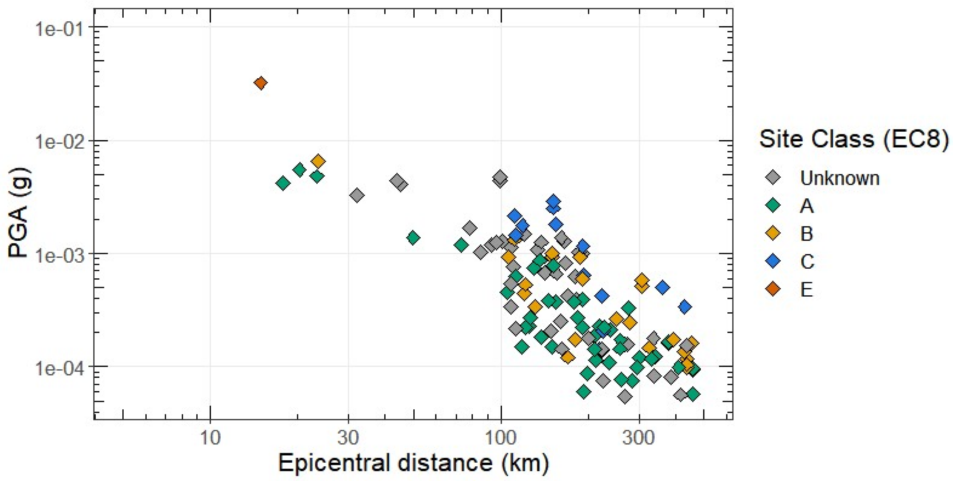

Figure 6: PGA (Peak Ground Acceleration) recorded at seismic stations during Le Teil earthquake as function of epicentral distance and site class (according to the EC8 classification).

Figure 7 shows the time histories recorded by this sensor.

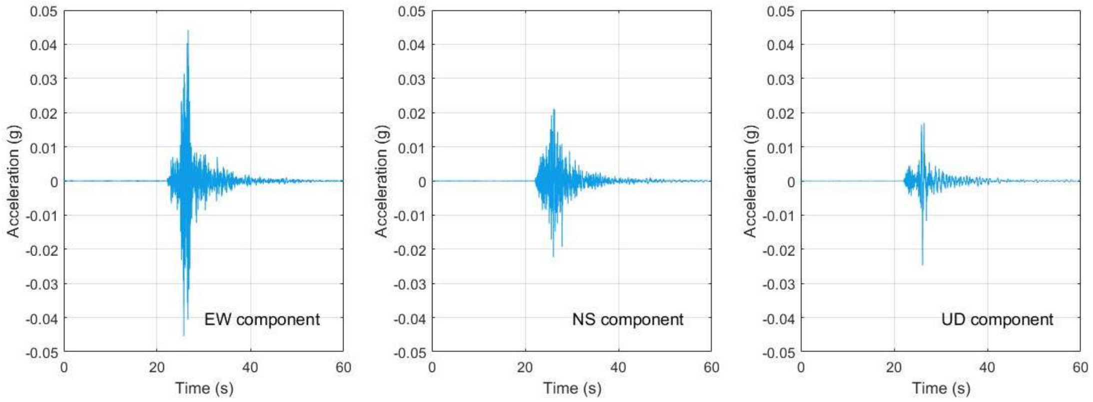

Figure 7: Time histories recorded at Cruas RAN free-field accelerometer.

The ground motion recorded at Cruas free field is characterized by a resonance peak around 9 Hz. This is related to the presence of a thin sediment layer (7 m thick) above stiff rock for the free-field surface condition (see more details in next sections).

2019/11/11 LE TEIL EARTHQUAKE: IMPACT ON CRUAS NPP (SHUTDOWN, INSPECTIONS AND RESTART)

This section describes the actions that were performed by the Cruas NPP operators and their engineering supports in a chronological manner, from the earthquake occurrence time until the restart of the units.

November 11th: Immediate actions by operators and decisions

According to French nuclear basic safety rule RFS I-3-b (ASN, 1984), a seismic recording system (called "EAU") is implemented on each NPP site. This system is triggered with a first threshold scaled to 0.01g that, when reached, simultaneously sends a warning message to operators (in main control room) and records acceleration time histories in 5 locations (free field, basemat of the reactor building, main floor at +20m in the reactor building, basemat of the nuclear auxiliary building and ASG tank building) for 3 components (X, Y and Z plant main axis).

At 11:53 am local time, seismic warning system appeared in main control room and operators immediately launched the seismic event operating procedure coded as "I-EAU", which mainly consist of i) confirming that an earthquake was felt by a large part of NPP staff, then ii) launching immediate plant walkdowns to identify any damage or any seismic-induced situation and finally iii) get and post-process seismic records from the five locations given above.

From 11:53 am to 4:00 pm local time, previous actions were implemented. No specific issues were reported by plant walkdown teams. However, one of the records (ASG tank building, vertical component) indicated that the maximum recorded acceleration was 0.037g, which exceeded the Inspection Earthquake threshold defined at 0.05g in horizontal direction and scaled at 0.033g (2/3 x 0.05g) in vertical direction. Due to this record and according to I-EAU procedure, the 3 units that were under operation when the earthquake occurred (Units 2 to 4) where manually shutdown by the operators. This was progressively done in the afternoon and evening of the same day.

From November 12th to November 20th: Post-earthquake walkdowns and conclusions

According to RFS I-3-b, in case of plant shutdown due to an earthquake, authorization of restarting the plant should be given by the regulator based on a detailed investigation report provided by the operator.

Then, post-earthquake investigations were performed by the operator and its engineering support following international guidelines (IAEA, 2011) and (EPRI, 2015). Despite the relatively low recorded seismic level and the absence of any seismic related issue from immediate plant walkdown which would have led to an immediate restart of the plant according to these previous references, post-earthquake walkdowns covered a large panel of SSCs, including safety-related and non-safety-related ones, civil structures, mechanical and electrical equipment and SSCs outside of the base-isolated structures. These investigations were documented, as illustrated in Figure 8.

Figure 8: Illustration of post-earthquake plant walkdown.

The conclusions of these extensive plant walkdowns, confirmed by a Peer Review, established that the earthquake did not induce any damaged to any of the SSCs of the plant. The detailed investigation report was sent to the French Regulator (ASN) on November 22.

From November 22nd to December 6th: Assessment by the Regulator

The French Regulator (ASN) and its Technical Support Organization (TSO) IRSN assessed the reports sent by the operator and performed their own plant walkdown. These actions led to some requests for clarifications that were addressed by the operator.

At the end of this process, authorization of restarting the plants was given by the French Regulator on December 6. Finally, Cruas units 2 to 4 progressively restarted between December 7 to 13.

EMPIRICAL AND NUMERICAL SIMULATIONS APPLIED TO THE TEIL EARTHQUAKE

Within the SIGMA2 project (https://www.sigma-2.net/), four different simulation techniques (two empirical and two physics-based techniques) were used to reproduce the Le Teil earthquake. The four simulation techniques are:

- The **Irikura recipe**: (Irikura and Miyake, 2011) a strong ground motion methodology mainly developed and used in Japan, which is based on a kinematic description of the source. This empirical technique is based on small events corrections to generate Empirical Green's Functions (EGFs) and on large event source definition using asperities representing the rupture slip distribution. The summation over the rupture area of the convolution between EGFs and elementary slip on the fault allows to simulate the Ground Motion of the large event.
- The **Dujardin et al. (2020) technique** that is similar to the Irikura recipe: ground motions of a large event are simulated by summing the recordings of small events. This technique differs from the previous technique in the summation and the slip distribution generation techniques.
- A **1D Physics-Based Simulation** : where ground motions are calculated through the tensor product between the tensors of the earthquake source and the Green's function of the medium (including the soil layers) crossed by the seismic waves (Fasan, 2017; Magrin, 2012; Panza et al., 2012). The technique has been successfully applied and validated against past events and available ground motion prediction equations (Fasan, 2017; Fasan et al., 2016; Hassan et al., 2020; Magrin et al., 2016; Panza et al., 2012).
- A **3D Physics-Based Simulation** using the open-source high-performance computer code SPEED (http://speed.mox.polimi.it/, Mazzieri et al., 2013). In order to increase the frequency resolution, the SPEED signals have been enriched a posteriori at high frequencies using a technique based on ANN trained on strong ground motion recordings (Paolucci et al. 2021a and 2021b).

The common assumptions used by the different techniques are summarized in Figure 5 (right).

The analysis of seismic ground motion parameters in both, time and frequency domains, was performed at 5 stations (ADHE, CRU1, OGLP, TRI2 and A192B) that recorded the main event and the aftershocks. Two of these stations (CRU1 and TRI2) are located next to the Cruas and Tricastin NPP, respectively. Figure 9 compares the Fourier Amplitude Spectra of acceleration time histories computed through the different simulations at the CRU1 and TRI2. Knowing that a perfect match between simulations and recordings cannot be reached, overall, the FAS simulated using the different techniques approach the observed ground motion features with different accuracy levels, depending on the frequency band and the considered technique. Empirical Green's function techniques are particularly good at reproducing specific features of site response (i.e. the 8-9 Hz amplification peak observed on ground motion recorded at CRU1 station EW component), because site-response features are included in the recordings used as EGF. Physic-based simulations, particularly the 3D approach, allow to well reproduce lower frequency patterns of observed ground motion (below 1 Hz), where EGF-based simulations perform worse due to the poor signal-over-noise ratios of the small events.

In additional to the Fourier spectrum, simulated ground motions are analyzed in the time domain using four ground motion intensity measures: the peak ground acceleration (PGA), the peak ground velocity (PGV), the Arias Intensity (AI) and the corresponding duration (D5-95).

In two different frequency bands: [1-10Hz] for the empirical techniques and [0.2-2Hz] for the PBS techniques, Figure 10 shows the Goodness of Fit (GoF) between simulated and recorded data, calculated for the five ground motion indicators (PGA, PGV, mean(|FAS|), AI and D5-95), for the three components of CRU1 and TRI2 stations. The GoF is defined as $log_{10}\left(\frac{Simulated}{Recorded}\right)$ and a GoF equal to 0 means excellent agreement between the recorded and simulated data.

The estimated GoF are sensitive to the GM indicator, the station and the azimuth. For selected stations, a non-negligible variability is found also between approaches belonging to the same class of methods (i.e. the two EGFs and the two PBSs), because of the assumptions and constraints at the basis of the approaches.

At TRI2 station, all methods show higher performance, with relatively a smaller variability. However, closer to the fault and located to the north-west of the fault, CRU1 exhibits a larger variability of results.

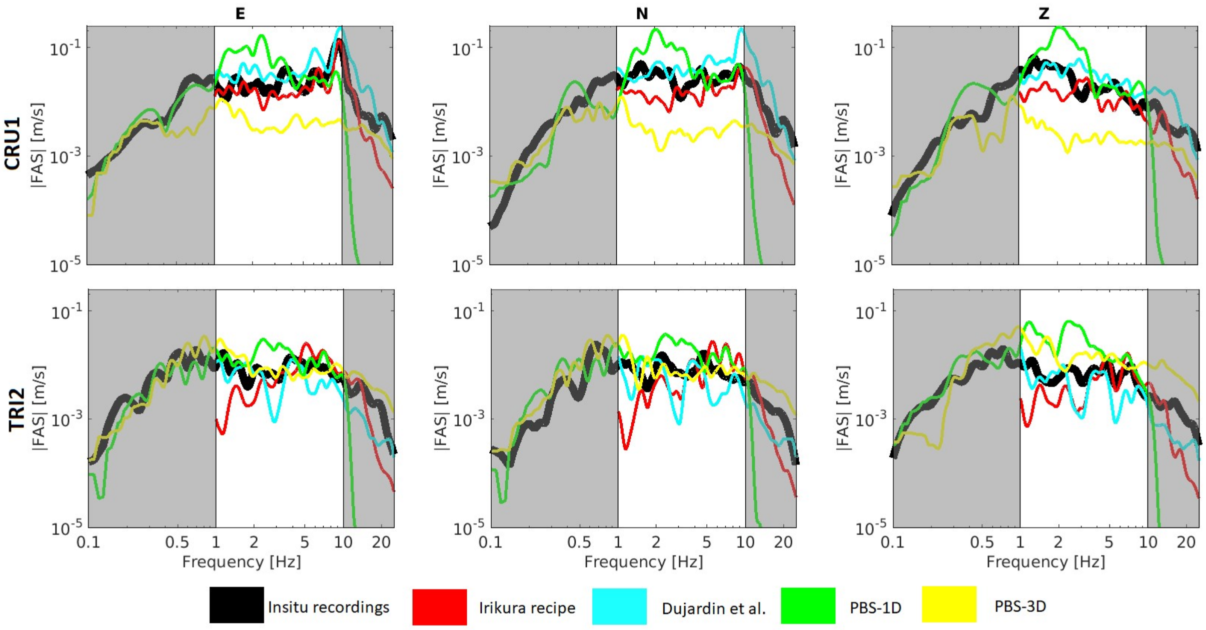

Figure 9: The Fourier Amplitude Spectrum (FAS) of three-component (E: East-West; N: North-South; Z: Up-Down) acceleration time histories calculated by the four different simulations (Irikura in red, Dujardin modified in cyan, PBS-1D in green, PBS-3D in yellow) and smoothed with the Konno and Ohmachi (b=40; Konno and Ohmachi, 1998), at CRU1 and TRI2. The thick black lines correspond to the recordings FAS.

The results of this simulation benchmark show that the different simulation techniques considered in this study are complementary to each other: while EGF-based simulations are reliable in the high frequency range (above 1 Hz), the 3D-physics-based simulations provide reliable ground motion in the low frequency range (below 2 Hz). The former techniques are limited by the availability and the quality of earthquake records to be used as EGF, while the latter techniques need to be complemented by other approaches in the higher frequency range. They can therefore be used to complement each other as hybrid simulations to obtain broad-band ground motion. Even more, 3D simulations could be used to generate synthetic Green's functions in regions where no small events are recorded.

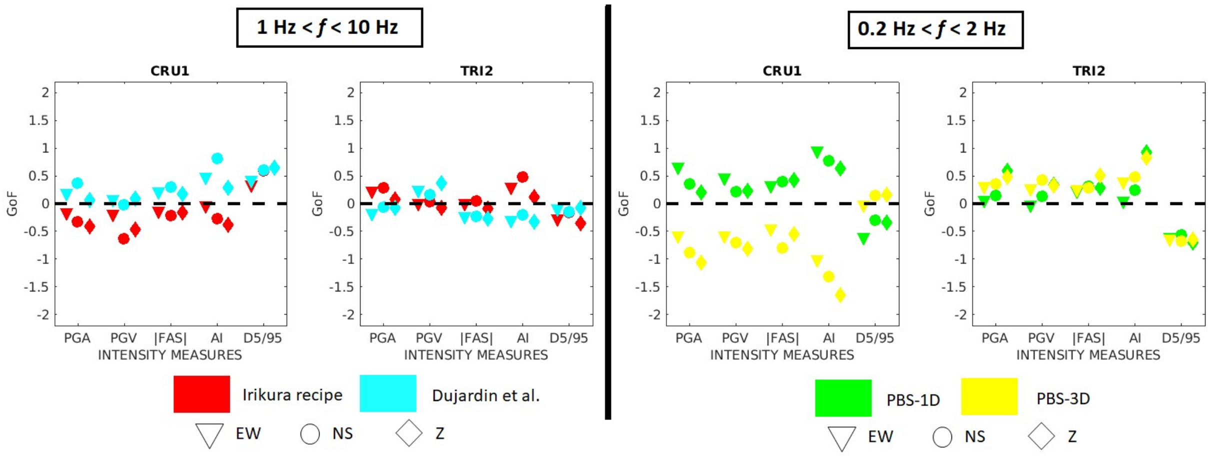

Figure 10: The Goodness of Fit (GoF) between simulated and recorded accelerograms calculated for the five ground motion intensity measures (PGA, PGV, FAS, Arias Intensity and Duration) estimated using the empirical techniques at high frequencies ([1-10Hz]) and the PBS techniques at low frequencies ([0.2-2Hz]). The results are shown for CRU1 and TRI2 stations in the 3 directions.

CURRENT STATUS OF ASSESSMENTS: STRUCTURAL BEHAVIOR AND SEISMIC RESPONSE OF THE PLANT

The locations of EAU sensors within Cruas NPP, inside or near Nuclear Island #1, are shown in Figure 11.

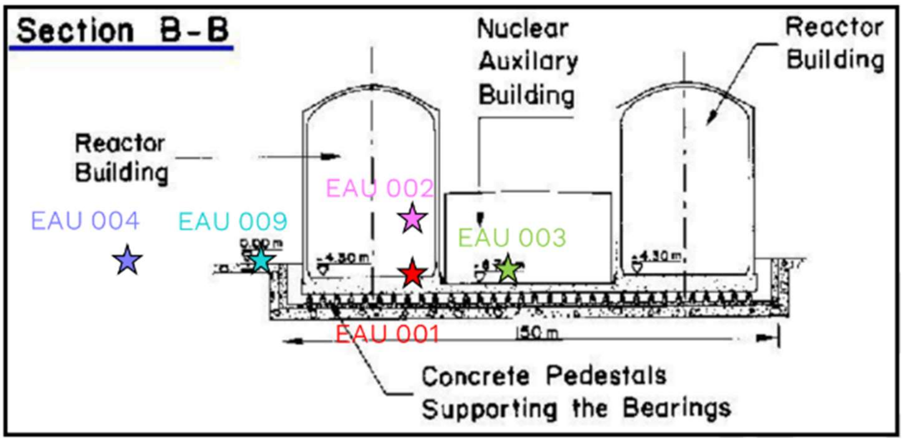

Figure 11: Location of EAU sensors within Cruas NPP.

The response spectra computed from the acceleration time histories registered at these positions, as well as the RAN sensor accelerations at free field conditions, are not presented in this paper because of the coming international benchmark (see conclusion) which will include a blind prediction phase. However, they highlight the frequency shift of the seismic signal within the isolated structure roughly between 1.5 and 1.8 Hz, whereas other sensors spectra display a rich frequency content between 5 and 15 Hz. This base-isolation effect is illustrated and commented in a different way in the next paragraphs.

Continuous wavelet transforms (Erlicher, 2007) were used to analyze the time histories frequency content. On RAN sensor time histories, the superficial alluvial layer mode located around 9 to 10 Hz is visible in Figure 12, as well as other frequencies, especially within the 5 to 15 Hz range.

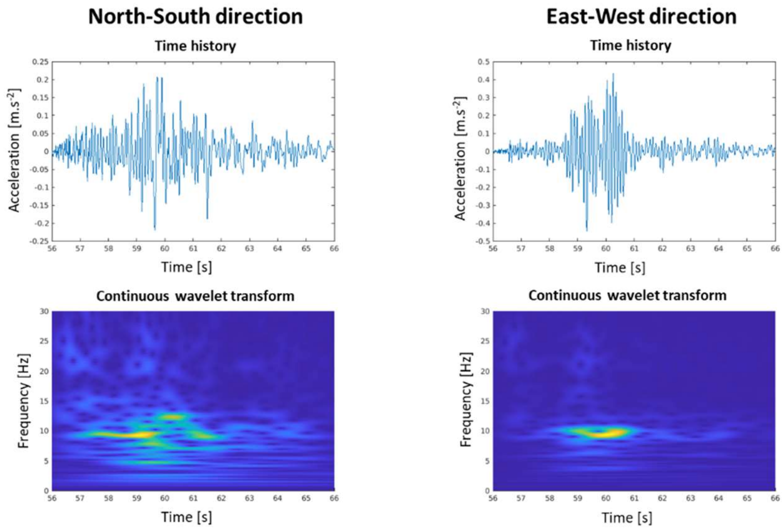

Figure 12: Frequency analysis of RAN sensor time histories, using continuous wavelet transform

Similar analysis applied to EAU sensors located within the isolated structure show a very different frequency content, with a single eigenfrequency highlighted in Figure 13 for the two sensors located within the lower levels, and still visible at +20m level even if other structural eigenfrequencies are visible in this case. The base isolation of the nuclear island has played a filter role, exactly as it was designed to behave, lowering the main eigenfrequency of the nuclear island to a very low value. Nevertheless, the vertical seismic movement is not filtered, and is responsible for both vertical and in some cases horizontal movements with higher frequencies within the higher levels, visible on EAU-002 time histories analysis.

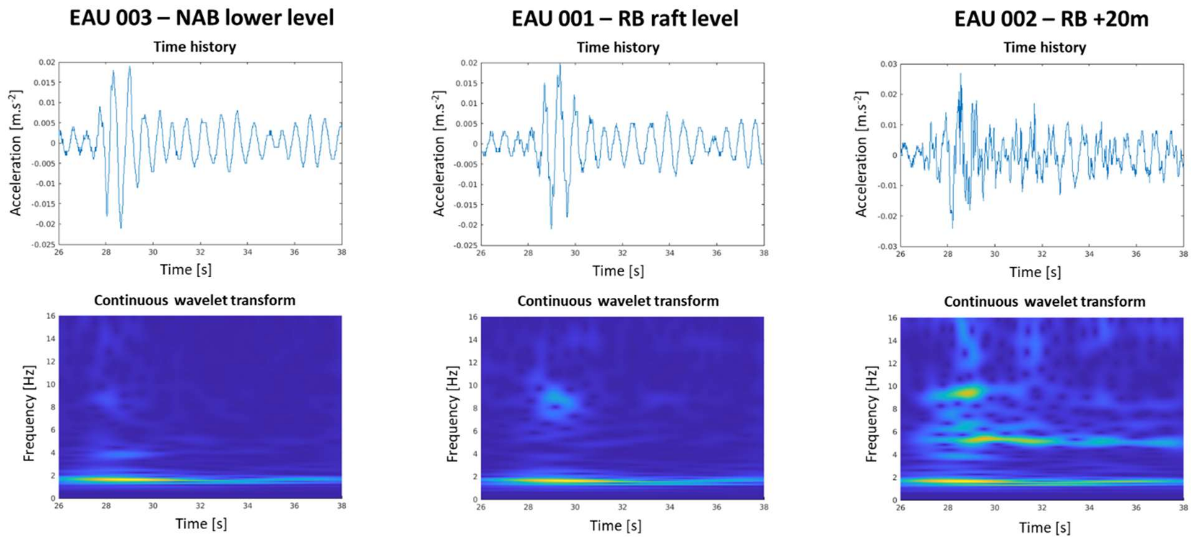

Figure 13: Frequency analysis of EAU 001 to 003 sensors' time histories in one horizontal direction, using continuous wavelet transform

Ridge detections techniques are used to follow up this frequency, which is shown to vary between 1.5 and 1.8 Hz during the main phase of the seismic motion, as shown in Figure 14. It is further plotted as a function of the acceleration level, as the neoprene bearings ensuring the base isolation are known to be slightly nonlinear, even at low amplitude. A least square regression is computed according to a power law, fitting rather well with the registered data from the 3 sensors, in the two horizontal directions. It is consistent with a main eigenfrequency varying between about 2 Hz at a very low level of excitation to around 1 Hz for earthquakes with an acceleration amplitude of about 10 times the ones recorded during Le Teil earthquake (Safe Shutdown Earthquake is defined at 0.3g PGA for Cruas site).

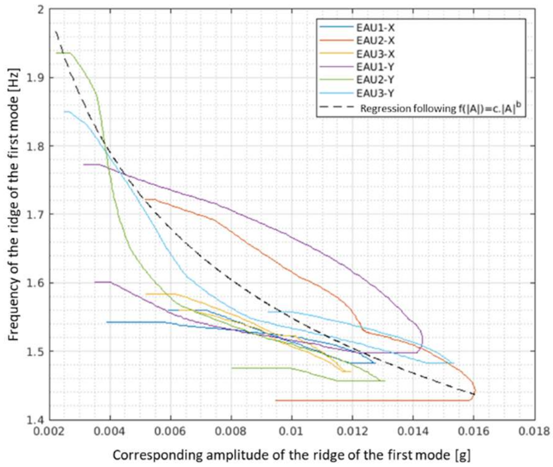

Figure 14: EAU 001 to 003 main ridge frequency follow-up as a function of the associated amplitude of the ridge

CONCLUSIONS AND PERSPECTIVES

Le Teil magnitude 4.9 (Mw) earthquake occurred on November 11, 2019 at approximately 15 km from Cruas NPP, a three-loop 900 MW Pressurized Water Reactor built on seismic base isolation. This earthquake led to a ground motion shaking between 0.02 and 0.05 g on site (Peak Ground Acceleration, free field). Although the ground motion level is not very high compared to the DBE of the Plant (0.3 g PGA), due to operational procedures, the plant was shut down and post-earthquake inspections were performed before restart. The conclusions of these extensive plant walkdowns, confirmed by a Peer Review, established that the earthquake did not induce any damaged to any of the SSCs of the plant. Finally, Cruas units NPP units progressively restarted less than one month after the event.

This seismic event, that was largely assessed and documented on the seismological aspect, also provides the ultimate missing piece of experience feedback regarding the actual behavior of a NPP built on seismic base isolation, in terms of dynamic behavior of the anti-seismic bearings themselves and in terms of dynamic behavior of the plant. This was achieved thanks to the records that allow to compare design studies that were performed 40 years ago to actual observations. Additional pieces of experience feedback, analyses and lessons learnt regarding this earthquake were also shared in the framework of the French Society for Nuclear Energy, (SFEN, 2020).

Finally, in order to move forward and to share this unique experience feedback with the largest community, EDF and IRSN have decided to organize an international benchmark. This benchmark, organized under the auspices of OECD/NEA, will include a first phase related to seismic ground motion characterization at Cruas site location and will also include a second phase related to assessing the seismic response of the plant including seismic base isolation system. EDF and IRSN are looking forward to share experience feedback with the largest international community in order to promote this optimized seismic design solution in the future, not only for current generations of plants but also for new ones such as SMRs or advanced reactors.

REFERENCES

ASN (1984). RFS I-3-b, Conception générale de la centrale et principes généraux applicables à l'ensemble de l'installation - Principes généraux de conception et d'installation - Instrumentation sismique. https://www.asn.fr/l-asn-reglemente/rfs/rfs-relatives-aux-rep/rfs-i-3.b.-du-08-06-1984

Causse, M., Cornou, C., Maufroy, E., Grasso, J. R., Baillet, L., & El Haber, E. (2021). Exceptional ground motion during the shallow M w 4.9 2019 Le Teil earthquake, France. *Communications Earth & Environment*, *2*(1), 1-9.

Cornou, C., Ampuero, J. P., Aubert, C., Audin, L., Baize, S., Billant, J., ... & Weng, H. (2020). Rapid response to the M_w 4.9 earthquake of November 11, 2019 in Le Teil, Lower Rhône Valley, France.

Delouis, B., Ampuero, J. P., Audin, L., Bernard, P., Brenguier, F., Grandin, R., ... & Voisin, C. Rapport d'évaluation du groupe de travail (GT) CNRS-INSU sur le séisme du Teil du 11 novembre 2019 et ses causes possibles, 2019 http://www.cnrs.fr/sites/default/files/ press_info/2019-12.*Rapport_GT_Teil_phase1_final_171219_v3. pdf (35 p., in french)*.

Delouis, B., Oral, E., Menager, M., Ampuero, J. P., Trilla, A. G., Régnier, M., & Deschamps, A. (2021). Constraining the point source parameters of the 11 November 2019 Mw 4.9 Le Teil earthquake using multiple relocation approaches, first motion and full waveform inversions. *Comptes Rendus. Géoscience*, *353*(S1), 1-24.

De Novellis, V., Convertito, V., Valkaniotis, S., Casu, F., Lanari, R., Monterroso Tobar, M. F., & Pino, N. A. (2020). Coincident locations of rupture nucleation during the 2019 Le Teil earthquake, France and maximum stress change from local cement quarrying. *Communications Earth & Environment*, *1*(1), 1-10.

Dujardin, A., Hollender, F., Causse, M., Berge-Thierry, C., Delouis, B., Foundotos, L., ... & Shible, H. (2020). Optimization of a simulation code coupling extended source (k− 2) and empirical green's functions: Application to the case of the middle durance fault. *Pure and Applied Geophysics*, *177*(5), 2255-2279.

Elmi, S., Busnardo, R., Clavel, B., Camus, G., Kieffer, G., Bérard, P., & Michaëly, B. (1996). Notice explicative, Carte Géologique France 1/50000, feuille Aubenas (865). *Orléans: BRGM*.

EPRI (2015). Guidelines for Nuclear Power Plant Response to an Earthquake. Report 3002005284. https://www.epri.com/research/products/3002005284

Erlicher, S., Argoul, P. (2007), Modal Identification of Linear Non-Proportionally Damped Systems by Wavelet Transform , Mechanical Systems and Signal Processing 21, no 3, pp. 1386-1421

Fasan, M., Magrin, A., Amadio, C., Romanelli, F., Vaccari, F., and Panza, G. F., 2016. A seismological and engineering perspective on the 2016 Central Italy earthquakes. *International Journal of Earthquake and Impact Engineering*, **1**(4), 395–420. DOI: 10.1504/IJEIE.2016.10004076

Fasan, M., 2017. *Advanced seismological and engineering analysis for structural seismic design*. Italy: University of Trieste.

Hassan, H. M., Fasan, M., Sayed, M. A., Romanelli, F., ElGabry, M. N., Vaccari, F., and Hamed, A., 2020. Site-specific ground motion modeling for a historical Cairo site as a step towards computation of seismic input at cultural heritage sites. *Engineering Geology*, **268**(April 2019), 105524. Elsevier. DOI: 10.1016/j.enggeo.2020.105524

IAEA (2011). Earthquake Preparedness and Response for Nuclear Power Plant. TECDOC-1905 https://www.iaea.org/publications/8473/earthquake-preparedness-and-response-for-nuclear-power-plants

IAEA (2020). Seismic Isolation Systems for Nuclear Installations. Safety Report Series n°66 https://www.iaea.org/publications/13646/seismic-isolation-systems-for-nuclear-installations

Irikura K., Miyake H. (2011) Recipe for predicting strong ground motion from crustal earthquake scenarios, *Pure Appl. Geophys*, DOI: 10.1007/s00024-010-0150-9.

Magrin, A., 2012. *Multi-scale seismic hazard scenarios*. Italy: University of Trieste.

Magrin, A., Gusev, A. A., Romanelli, F., Vaccari, F., and Panza, G. F., 2016. Broadband NDSHA computations and earthquake ground motion observations for the Italian territory. *International Journal of Earthquake and Impact Engineering*, **1**(1/2), 28. DOI: 10.1504/IJEIE.2016.10000979

Mordret, A., Brenguier, F., Causse, M., Boué, P., Voisin, C., Dumont, I., ... & Ampuero, J. P. (2020). Seismic stereometry reveals preparatory behavior and source kinematics of intermediate-size earthquakes. *Geophysical research letters*, *47*(17), e2020GL088563.

Mazzieri, I, Stupazzini M, Guidotti R, Smerzini C (2013) SPEED: SPectral Elements in Elastodynamics with Discontinuous Galerkin: a non-conforming approach for 3D multi-scale problems. Int J Numer Meth Eng 95(12):991–1010.

Paolucci, R., I. Mazzieri, G. Piunno, C. Smerzini, M. Vanini, and A. G. Özcebe (2021a). Earthquake ground motion modelling of induced seismicity in the Groningen gas field, Earthq. Eng. Struct. Dynam. 50, 135–154, doi: 10.1002/eqe.3367.

Paolucci, R., C. Smerzini, and M. Vanini (2021b). BB-SPEEDset: A Validated Dataset of Broadband Near-Source Earthquake Ground Motions from 3D Physics-Based Numerical Simulations, Bull. Seismol. Soc. Am. XX, 1–19, doi: 10.1785/0120210089

Panza, G. F., Mura, C. La, Peresan, A., Romanelli, F., and Vaccari, F., 2012. Seismic Hazard Scenarios as Preventive Tools for a Disaster Resilient Society (pp. 93–165). DOI: 10.1016/B978-0-12-380938-4.00003-3

RESIF (1995a). RESIF-RAP French Accelerometric Network, doi: 10.15778/RESIF.RA.

RESIF (1995b) RESIF-RLBP French Broad-band network, RESIF-RAP strong motion network and other seismic stations in metropolitan France, doi: 10.15778/RESIF.FR.

Ritz, J. F., Baize, S., Ferry, M., Larroque, C., Audin, L., Delouis, B., & Mathot, E. (2020). Surface rupture and shallow fault reactivation during the 2019 Mw 4.9 Le Teil earthquake, France. *Communications Earth & Environment*, *1*(1), 1-11.

SFEN (2020). Resilience of nuclear power plants to seismic risk: case study of the Le Teil earthquake https://www.sfen.org/avis/la-resilience-des-centrales-nucleaires-au-risque-sismique-cas-du-seisme-du-teil/

Sira, C., Schlupp, A., Maufroy, E., Provost, L., Dretzen, R., Bertrand, E., ... & Schaming, M. (2020). *Rapport macrosismique n 4, Séisme du Teil (Ardèche) 11 novembre 2019 à 11 h 52 locale, Magnitude 5, 2 ML (RENASS), Intensité communale max VII-VIII (EMS98)*. BCSF-RENASS-2020-R2. https://doi. org/10.13140/RG. 2.2. 27570.84166.